ON THE ONSET OF DETONATION IN A NONUNIFORMLY HEATED GAS

Ya. B. Zel'dovich, V. B. Librovich,
G. M. Makhviladze, and G. I. Sivashinskii

Investigation of detonation waves in gases is usually carried out by means of shock tubes in which detonation is initiated either by a shock wave or an accelerating flame with the initial temperature of the combustible mixture close to ambient. The actual generation of a detonation wave in such tests is readily ascertained by the rapid change of pressure or temperature, since detonation increases the chemical reaction rate severalfold.

Conditions in an internal combustion engine in the presence of "knock" are different. Owing to preliminary compression of combustible gas mixed with products of combustion remaining in the cylinder after the exhaust stroke, the gas temperature can be sufficiently high to create favorable conditions for an explosion-like chemical reaction throughout the cylinder volume. If the temperature and the mixture are uniform throughout the cylinder volume, the chemical reaction will result in a uniform pressure rise there. If, on the other hand, the temperature of the combustible mixture varies from point to point, the chemical reaction at these proceeds differently, and this leads to an uneven expansion of gas and a possible initiation of shock and detonation waves. Unlike conventional detonation experiments in shock tubes, the exact determination of the point of transition of the chemical reaction from a uniform explosion-like mode to that of a spreading detonation wave is a difficult experimental task necessitating precision measurements.

A theoretical study of this problem is presented here. The problem of detonation onset in a nonuniformly heated gas susceptible to chemical reaction is solved. Three reaction modes are shown to be possible. If the temperature distribution at the initial instant of time is such that the gas is nearly uniformly heated, the reaction mode is that of a thermal explosion. With a steep temperature distribution, a detonation wave detached from the reaction wave is generated. Finally, there is a temperature distribution such that the generated detonation wave becomes capable of initiating a reaction, and a stationary detonation mode sets in.

1. Statement of Problem. Let at the initial instant of time the temperature profile of a reactive gas in the half-space $X > 0$ be given in the form of the linear function

$$T(0, X) = T_0 - \varkappa X \tag{1.1}$$

It is also assumed that the gas pressure P and the relative concentration a of the combustible constituent [fuel] are constant and that the gas is at rest, i.e.,

$$P(0, X) = P_0, \qquad U(0, X) = 0, \qquad a(0, X) = 1 \tag{1.2}$$

where U(t, X) is the velocity of gas.

To satisfy the condition $T(t, X) \geq 0$ (for $0 \leq t < \infty$), we assume that $T(0, X) = 0$ for $X > T_0/\varkappa$. If we confine ourselves to the initial stage of perturbation onset (that this is sufficient will be shown in the following), the later condition will not be restrictive owing to the finiteness of the propagation velocity of these.

The gas is assumed to be perfect, i.e., its equation of state is of the form

$$PV = RT \tag{1.3}$$

Moscow. Translated from Zhurnal Prikladnoi Mekhaniki i Tekhnicheskoi Fiziki, Vol. 11, No. 2, pp. 76–84, March-April, 1970. Original article submitted April 25, 1969.

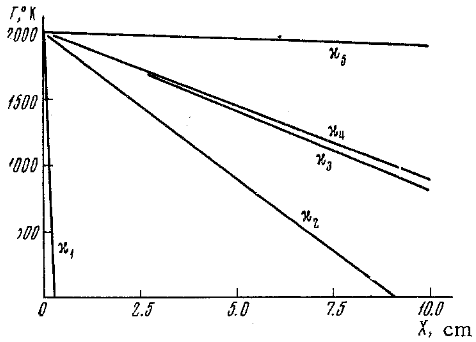

Fig. 1

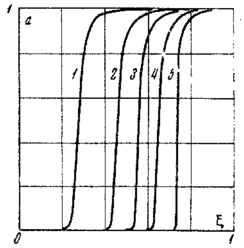

Fig. 2a

Here R is the gas constant and V is the specific volume of gas.

The statement of the problem implies a stationary initial state of the perfect inert gas, i.e., that the initial state of the latter is changed only by the incipient chemical reaction which must set the gas in the vessel into motion. Since at the hot wall the reaction develops with greater intensity, a rapid expansion of gas takes place there, and the onset of a shock wave becomes possible. Under certain conditions, this wave may develop into a detonation wave.

Various chemical reaction modes are possible, depending on the specified initial temperature gradient.

For considerable $\varkappa$, the reaction induction time also decreases, and layers of gas further removed from the hot wall begin to play an increasingly important role in the formation of the shock wave. The latter becomes sufficient for initiating a reaction in the gas, which will then proceed in a detonation mode.

For small $\varkappa$ (nearly uniformly heated gas), the reaction develops throughout the whole vessel without shocks.

2. Equations and Boundary Conditions. We use one-dimensional equations of gasdynamics for analyzing the motion of gas and take into consideration the energy released by the chemical reaction (for simplicity, the latter is considered to be of the first order with respect to a):

$$\frac{\partial\rho}{\partial t}+\frac{\partial\rho U}{\partial X}=0 \quad \left(\rho=\frac{1}{V}\right), \qquad \frac{\partial U}{\partial t}+U\frac{\partial U}{\partial X}=-\frac{1}{\rho}\frac{\partial P}{\partial X}$$

$$\frac{\partial P}{\partial t}+U\frac{\partial P}{\partial X}+\gamma P\frac{\partial U}{\partial X}=(\gamma-1)\,Qa\rho ke^{-E/RT}, \qquad \frac{\partial a}{\partial t}+U\frac{\partial a}{\partial X}=-kae^{-E/RT} \tag{2.1}$$

Here Q is the heat energy release, E is the activation energy, k is the preexponential factor, and γ is the adiabatic exponent.

It is convenient to pass in the subsequent analysis to the Lagrangian coordinate x and dimensionless variables defined by the following equations:

$$P=P_0p, \qquad T=T_0\theta, \qquad U=\sqrt{\gamma RT_0}\,u, \qquad V=\frac{RT_0}{P_0}v$$

$$t=\frac{\tau}{k}\exp\frac{E}{RT_0}, \qquad \varkappa=\frac{\lambda kT_0}{\sqrt{\gamma RT_0}}\exp\left(-\frac{E}{RT_0}\right)$$

$$x\frac{P_0\sqrt{\gamma RT_0}}{kRT_0}\exp\frac{E}{RT_0}=\int_0^X\frac{dX}{V(t,X)} \tag{2.2}$$

$$X=\xi\frac{\sqrt{\gamma RT_0}}{k}\exp\frac{E}{RT_0}$$

The equations of motion (2.1) then become

$$\frac{1}{\gamma-1}\frac{\partial\theta}{d\tau}+p\frac{\partial u}{\partial x}=\alpha a\exp\left[\beta\left(1-\frac{1}{\theta}\right)\right], \qquad \gamma\frac{\partial u}{\partial\tau}+\frac{\partial p}{\partial x}=0$$

$$\frac{\partial a}{\partial\tau}+a\exp\left[\beta\left(1-\frac{1}{\theta}\right)\right]=0, \qquad \frac{\partial\xi}{\partial\tau}=u, \qquad \frac{\partial\xi}{\partial x}=v \tag{2.3}$$

$$\left(\alpha=\frac{Q}{RT_0}, \quad \beta=\frac{E}{RT_0}\right)$$

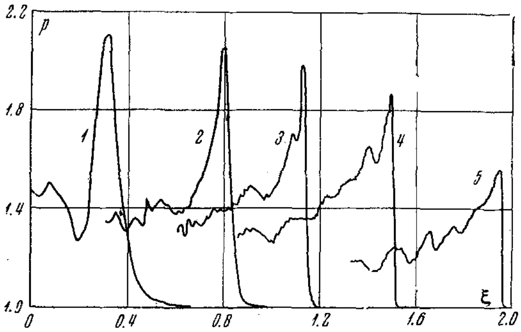

Fig. 2b

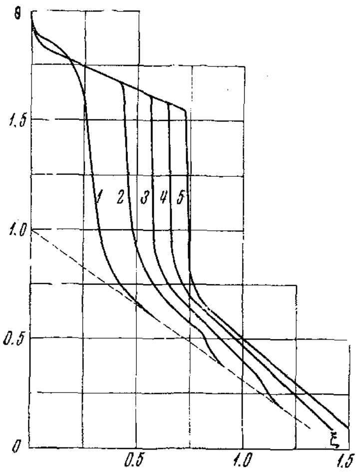

Fig. 2c

Initial conditions (1.1) and (1.2) and the equation of state (1.3) after transformation take the form

$$\theta(0,\ x) = e^{-\lambda x}\ (\theta(0,\ \xi) = 1 - \lambda\xi),\quad v(0,\ x) = \theta(0,\ x)$$
$$\xi(0,\ x) = \lambda^{-1}(1 - e^{-\lambda x}),\quad p(0,\ x) = 1,\quad a(0,\ x) = 1,\quad u(0,\ x) = 0, \tag{2.4}$$
$$pv = \theta$$

Note that a symmetric extension of function T(0, X) into region X < 0, reduces this problem to that of Cauchy.

3. Progamming Calculations for the Computer. Numerical integration of system (2.3) with initial conditions (2.4) makes it necessary to consider the problem on a finite segment of the x axis. To comply with this we introduce a wall at x = L. The boundary conditions (conditions of impermeability of walls) are then written

$$u(\tau,\ 0) = u(\tau,\ x^{(0)}) = 0$$
$$x^{(0)} = -\frac{1}{\lambda}\ln(1 - \lambda\xi^{(0)}),\quad \xi^{(0)} = \frac{kL}{\sqrt{\gamma RT_0}}\exp\left(-\frac{E}{RT_0}\right) \tag{3.1}$$

The boundary condition at the cold wall, introduced for bounding the region of integration, does not affect the course of the reaction, since we are interested in times shorter than that required for the shock wave to reach the right-hand boundary.

Since the appearance of shocks is to be expected, we introduce into the solution of the problem an artificial viscosity, as was done by Neuman and Richtmayer [1]. This permits the substitution of a thin transition layer for the shock in which the parameters, although rapidly changing, are free of discontinuities. The introduction of artificial viscosity makes it possible to avoid involved calculation of shock by the Hugoniot equation. The artificial viscosity is defined by the following equation:

$$q = \gamma\frac{(\nu\Delta x)^2}{v}\left(\frac{\partial u}{\partial x}\right)^2 \text{ for } \frac{\partial u}{\partial x} < 0;\ q = 0 \text{ for } \frac{\partial u}{\partial x} \geqslant 0 \tag{3.2}$$

where Δx is the increment along the space coordinate and ν is the coefficient of artificial viscosity.

The first two equations of (2.3) are now replaced by

$$\frac{1}{\gamma-1}\frac{\partial\theta}{\partial\tau} + (p+q)\frac{\partial u}{\partial x} = \alpha a\exp\left[\beta\left(1 - \frac{1}{\theta}\right)\right]$$
$$\gamma\frac{\partial u}{\partial\tau} + \frac{\partial}{\partial x}(p+q) = 0 \tag{3.3}$$

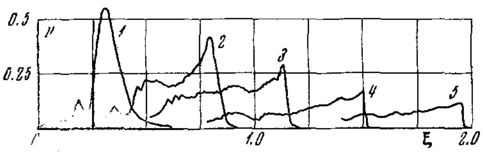

Fig. 2d

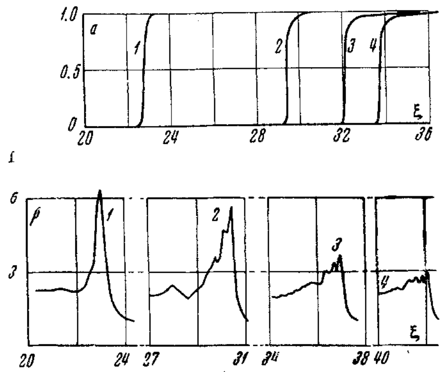

Fig. 3

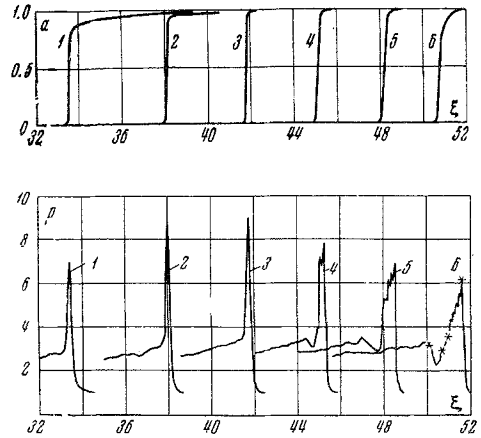

Fig. 4a, b

Using the difference method of the "tripod" type [2], we readily obtain for the solution of our problem the following explicit algorithm:

$$u_j^{n+1} = u_j^n - \frac{(\Delta\tau)_n}{\gamma\Delta x}\left(p^n_{j+1/2} + q^n_{j+1/2} - p^n_{j-1/2} - q^n_{j-1/2}\right)$$

$$\xi_j^{n+1} = \xi_j^n + (\Delta\tau)_n u_j^{n+1}, \quad v_j^{n+1} = (\Delta x)^{-1}\left(\xi^{n+1}_{j+1/2} - \xi^{n+1}_{j-1/2}\right)$$

$$a_j^{n+1} = a_j^n\,[1 + (\Delta\tau)_n f(\theta_j^n)]^{-1}, \quad f(\theta_j^n) = \exp\left[\beta\left(1 - \frac{1}{\theta_j^n}\right)\right]$$

$$p_j^{n+1} = \frac{(\gamma-1)^{-1}\theta_j^n + (\tfrac{1}{2}p_j^n + q_j^n)(v_j^n - v_j^{n+1}) + \alpha(a_j^n - a_j^{n+1})}{\tfrac{1}{2}\left[(\gamma+1)(\gamma-1)^{-1}v_j^{n+1} - v_j^n\right]} \tag{3.4}$$

$$\theta_j^{n+1} = p_j^{n+1} v_j^{n+1}$$

$$q_j^n = \frac{2\gamma\nu^2}{v_j^n}\left(u^n_{j+1/2} - u^n_{j-1/2}\right)^2 \text{ for } u^n_{j+1/2} < u^n_{j-1/2}; \quad q_j^n = 0 \text{ for } u^n_{j+1/2} \geqslant u^n_{j-1/2}$$

$$0 \leqslant j \leqslant J \quad (J\Delta x = x^{(0)}), \quad 0 \leqslant n < \infty$$

Here φ_j^n denotes the value of function φ at the instant of time $(\Delta\tau)_1 + (\Delta\tau)_2 + \ldots + (\Delta\tau)_n$ at point $j\Delta x$; the time-increment $(\Delta\tau)_n$ is chosen on the basis of Courant's stability condition

$$(\Delta\tau)_n = \frac{\Delta x\,\sqrt{\gamma/2\nu}}{\max_j \sqrt{\theta_j^n / v_j^n}} \tag{3.5}$$

which controls the accumulation of small errors in the calculation.

The boundary and initial values of parameters are calculated by the following equations:

a) boundary conditions

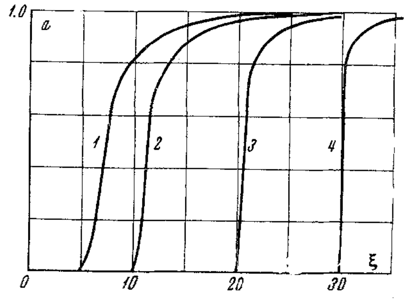

Fig. 5

$$u_0^{n+1} = \xi_0^{n+1} = u_J^{n+1} = q_0^{n+1} = q_J^{n+1} = 0, \quad \xi_J^n = \xi^{(0)}$$

$$a_J^n = a_J^{n-1}\,[1 + (\Delta\tau)_{n-1} f(\theta_J^{n-1})]^{-1}$$

$$a_0^n = a_0^{n-1}\,[1 + (\Delta\tau)_{n-1} f(\theta_0^{n-1})]^{-1}$$

$$v_J^n = v_J^{n-1} - \frac{(\Delta\tau)_{n-1}}{\Delta x} u_{J-1}^{n-1}, \quad p_J^n = \frac{\theta_J^n}{v_J^n}$$

$$v_0^n = v_0^{n-1} + \frac{(\Delta\tau)_{n-1}}{\Delta x} u_1^{n-1}, \quad p_0^n = \frac{\theta_0^n}{v_0^n} \tag{3.6}$$

$$\theta_J^n = \theta_J^{n-1} + (\Delta\tau)_{n-1}(\gamma-1)\alpha a_J^n f(\theta_J^{n-1}) + (\gamma-1)\frac{(\Delta\tau)_{n-1}}{\Delta x} u_{J-1}^{n-1}\left(p_J^{n-1} + q_J^{n-1}\right)$$

$$\theta_0^n = \theta_0^{n-1} + (\Delta\tau)_{n-1}(\gamma-1)\alpha a_0^n f(\theta_0^{n-1}) - (\gamma-1)\frac{(\Delta\tau)_{n-1}}{\Delta x} u_0^{n-1}\left(p_0^{n-1} + q_0^{n-1}\right)$$

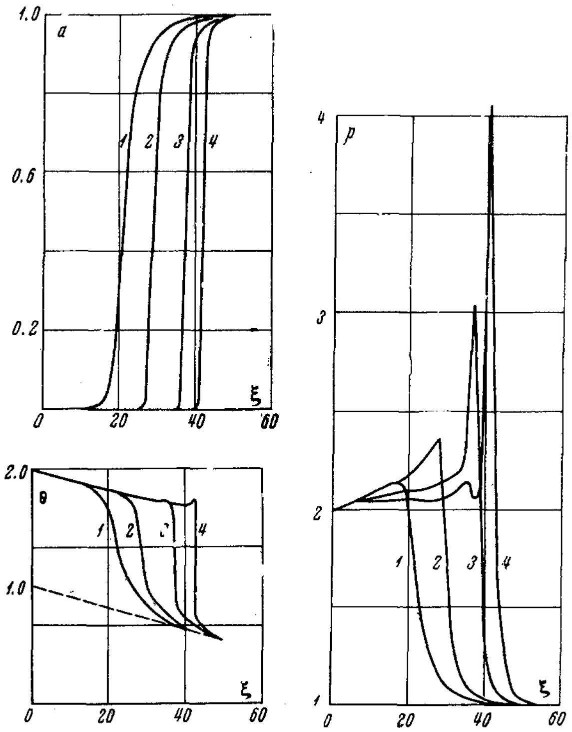

Fig. 6a, b, c

b) initial conditions

$$\theta_j^0 = \exp(-\lambda j \Delta x), \quad \xi_j^0 = \lambda^{-1}[1 - \exp(-\lambda j \Delta x)]$$
$$p_j^0 = a_j^0 = 1, \quad u_j^0 = 0, \quad v_j^0 = \theta_j^0 \qquad (3.7)$$

4. Discussions. The following values of dimensionless parameters were used in calculations: ν = 1.7, J = 350, α = 5, β = 10, γ = 1.2, $\xi^{(0)}$ = 55.

In the following, the results are given in physical variables for k - 10^{10} sec^{-1}, T_0 = 2000°K, and L = 10 cm.

We also choose λ_1 = 0.66 ($\varkappa_1$ = 7360 deg/cm), λ_2 = 0.02 ($\varkappa_2$ = 220), λ_3 = 0.017 ($\varkappa_3$ = 118), λ_4 = 0.01 ($\varkappa_4$ = 110), and λ_5 = 0.001 ($\varkappa_5$ = 11).

The initial temperature distribution for these values of $\varkappa$ are shown in physical variables in Fig. 1.

First, let us consider the case of considerable temperature gradients (λ_1 = 0.66). The distribution of parameters a, p, θ, and u along the coordinate is shown in Fig. 2a-d where curves 1, 2, 3, 4, and 5 relate to instants of time τ = 0.41, 0.82, 1.22, 2.44, and 3.93.

At τ = 0.41 the reaction and the shock waves coincide (Fig. 2a, b). The distance between the two waves increases at an increasing rate with time, and the shock wave becomes detached from that of the reaction.

A pulsating pressure behind the shock wave can be seen in Fig. 2b. Small amplitude pulsations (ripples) and large scale oscillations, representing acoustic perturbations propagating behind the shock-wave front, can be distinguished there.

The small pressure oscillations at the wave profile are due to the finite-difference construction of the algorithm (3.4). The magnitude of these pulsations determines the accuracy which can be reasonably expected from these calculations. The maximum intensity of the shock wave is $p/p_0 \approx 2.1$. After the separation of the shock wave from that of the reaction, the former becomes attenuated owing to the rarefaction waves (troughs in the wave profile) overtaking the shock wave.

Initial temperature distribution is shown in Fig. 2c by a dashed line. It is seen that the increase of temperature is essentially due to the reaction wave, while the heating of gas by the shock wave is insignificant, hence the slowing down of the reaction (Fig. 2a). Had the equations contained terms related to diffusion and thermal conductivity, a normal flame propagation would have resulted. Note that the shock wave velocity is somewhat higher than the normal rate of flame propagation; hence, the absence of these terms does not affect the formation and propagation of the shock wave.

Variation of the gas velocity relative to the walls with time is shown in Fig. 2d.

The same reaction mode is obtained for λ_2 = 0.02. The behavior of parameters a and p are shown in Fig. 3, where curves 1, 2, 3, and 4 relate to times τ = 7.44, 11.49, 16.65, and 22.15.

The difference between this and the previous case is that [here] the shock wave becomes detached from the reaction wave much later and at considerably greater distances from the hot wall (even at τ = 7.44 and ξ = 23.0 the two are still together), owing to the greater mass of combustion products taking part in generating the shock wave. This also explains the considerably higher intensity of the shock wave – in this case equal to 6.6 – than in the previously considered case.

The course of the reaction in a detonation mode is shown in Fig. 4a, b. In this case λ_3 = 0.0107 is that critical gradient λ_1^* at which detonation occurs. The results of solution are presented in the form of curves 1, 2, 3, 4, 5, and 6 which relate, respectively, to times τ = 5.73, 7.84, 9.53, 11.23, 12.96, and 14.76. The wave velocity can be calculated from the data of Fig. 4; for the above time intervals, it is 15.07, 5.57, 5.80, 5.29, 4.88, and 4.53, respectively (these velocities are normalized with respect to the speed of sound at 300° K).

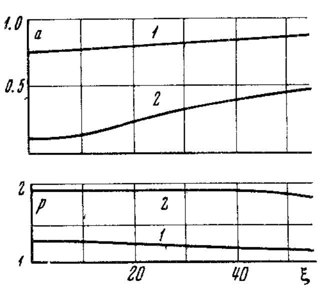

Fig. 7

On the other hand, from the equation for a strong detonation wave [3];

$$D = \sqrt{2(\gamma^2 - 1)Q} \tag{4.1}$$

where D is the detonation wave velocity, we find that D = 4.95.

At the instant of time τ = 14.76 the detonation wave mode apparently changes to that of the Chapman–Jouguet. This is confirmed by the calculation of the detonation wave velocity with respect to the products of combustion, which is equal to the local speed of sound. These calculations were made for points denoted in Fig. 4b by asterisks. The parameter (D – w)/c, where w is the velocity of products of combustion at a given point and c is the speed of sound at the same point, is equal to 0.97, 1.06, 0.98, and 0.53 (in order of increasing ξ). The last of these relates to the point at which the reaction has not yet begun. Deviations of these values from unity are within the limits of accuracy of determination of the shock wave velocity.

The discrepancy between the values of wave velocity obtained by numerical calculation and derived from Eq. (4.1) can be explained by the instability of the detonation wave. This was noted in [4-6] in which the instability of one-dimensional propagation of detonation waves was investigated. Pressure pulsations observed in [5, 6] were also noted by us (results of these investigations are not presented here). We would only note that, unlike in the case considered here, the detonation wave velocity and the supercompression ratio in [5, 6] were determined by external conditions – the motion of a piston.

It should be recalled that the propagation of the wave itself is to a certain extent arbitrary, owing to its instability with respect to spatial perturbations. The experimentally observed detonation waves have a complex three-dimensional nonstationary structure. Hence, only the first stage of detonation wave formation can be illustrated prior to its acquiring a spatial structure.

Let us compare these results with the propagation of a reaction in an incompressible gas. Setting in Eqs. (2.3) $\partial u/\partial x = 0$, we readily obtain

$$e^{\beta}\tau = Ei\left[\frac{\beta}{\Delta - a\sigma}\right] - Ei\left[\frac{\beta}{\Delta - \sigma}\right] + e^{\beta/\Delta}\left\{Ei\left[\frac{\beta\sigma}{\Delta(\Delta - \sigma)}\right] - Ei\left[\frac{\beta a\sigma}{\Delta(\Delta - \sigma a)}\right]\right\}$$
$$\left(\sigma = \alpha(\gamma - 1),\ \Delta = 1 + \sigma - \lambda\xi,\ Ei[x] = \int_{-\infty}^{x} \frac{e^z\,dz}{z},\quad x > 0\right) \tag{4.2}$$

defining the time-dependence of concentration a.

The results of calculation by Eq. (4.2) are shown in Fig. 5, where curves 1, 2, 3, and 4 relate to instants of time τ = 0.27, 0.42, 1.34, and 6.75 (λ_3 = 0.0107).

The pattern of detonation wave formation can be observed in Figs. 6a-c (λ_4 = 0.01), where curves 1, 2, 3, and 4 relate to instants of time τ = 1.55, 3.10, 7.75, and 10.75. At the beginning the variation of all parameters is fairly smooth, then with the progress of wave formation the gradients become more and more steep. Here the wave is formed later than in the previous case.

If the slope of the temperature profile is further decreased, then, from λ_2^* = 0.003 onwards, the reaction takes place throughout the whole vessel, i.e., in the mode of a thermal explosion.

We would point out that the critical gradients λ_1^* and λ_2^* are functions of the length of the vessel. When this length is shorter than the distance at which transition to the Chapman–Jouguet mode occurs, the mode of the chemical reaction can be classified as a thermal explosion.

Solutions for λ_5 = 0.001 are shown in Fig. 7, where curves 1 and 2 relate to instants of time τ = 0.18 and 0.34. The complete burnup of the combustible constituent is achieved at the instant of time τ = 0.47. Pressure in the vessel rises nearly uniformly to $2P_0$. This is readily derived from the system of Eqs. (2.1) by equating to zero the derivatives with respect to x.

5. Knock in Internal Combustion Engines. The explosion-like combustion occuring in internal combustion engines is referred to as knock. It is usual at present to explain this phenomenon in terms of kinetic concepts. Conclusions reached by various authors are to a great extent contradictory and do not adequately explain the accumulated experimental data. A detailed survey of current views on this subject was made in the monographs [7, 8]. The recent paper [9] should also be noted.

The explanation of this phenomenon on purely thermal grounds, as proposed in this paper, is based on the assumption that a detonation wave can be generated by the uneven heat distribution in the reactive gas mixture. The reason for the considerable thermal and mechanical overloading of an engine working under knocking conditions is explained by the presence of detonation waves. For example, in the case of $\lambda_3 = 0.0107$, the detonation wave intensity is ~ 6. According to the formula for detonation wave reflection from a solid wall [10], the pressure behind such a wave is ~ 15 P_0.

Occurrence of detonation waves under knock conditions had been experimentally observed, and is described in [8].

The authors wish to express their deep gratitude to L. A. Chudov for his considerable help in solving this problem.

LITERATURE CITED

1. I. Neuman and R. Richtmayer, "A method for the numerical calculation of hydrodynamic shocks," J. Appl. Phys., 21, No. 3, 1950.
2. R. D. Richtmayer, The Difference Method for Solving Boundary Problems [Russian translation], Izd. Inostr. Lit., Moscow, 1960.
3. Ya. B. Zel'dovich and A. S. Kompaneets, Theory of Detonation [in Russian], Gostekhizdat, Moscow, 1955.
4. P. M. Zaidel and Ya. B. Zel'dovich, "One-dimensional instability and attenuation of detonation," PMTF, No. 6, 1963.
5. W. Fickett and W. W. Wood, "Flow calculations for pulsating one-dimensional detonations," Phys. Fluids, 9, No. 5, 1966.
6. J. J. Eerpenbeck, "Nonlinear theory of unstable one-dimensional detonations," Phys. Fluids, 10, No. 2, 1967.
7. V. Jost, Explosion and Combustion in Gases [Russian translation], Izd. Inostr. Lit., Moscow, 1952.
8. A. S. Sokolik, Spontaneous Ignition, Flame, and Detonation in Gases [in Russian], Izd. AN SSSR, 1960.
9. W. S. Affleck and A. Fish, "Knock: flame acceleration or spontaneous ignition?" Combust. and Flame, 12, No. 3, 1968.
10. L. D. Landau and E. M. Lifshits, Mechanics of Continuous Media [in Russian], Gostekhizdat, 1954.